

FPGA Design Space Exploration for Scientific HPC Applications Using a Fast and Accurate Cost Model Based on Roofline Analysis

Syed Waqar Nabi^{a,*}, Wim Vanderbauwhede^a

^a*School of Computing Science, University of Glasgow, Glasgow G12 8QQ, UK.
T:+44 (0) 141 330 2074.*

Abstract

High-performance computing on heterogeneous platforms in general and those with FPGAs in particular presents a significant programming challenge. We contend that compiler technology has to evolve to automatically optimized applications by transforming a given original program. We are developing a novel methodology based on *type transformations* on a *functional* description of a given scientific kernel, for generating *correct-by-construction* design variants. An associated lightweight costing mechanism for evaluating these variants is a cornerstone of our methodology, and the focus of this paper. We discuss our use of the *roofline model* to work with our optimizing compiler to enable us to quickly derive accurate estimates of performance from the design's representation in our custom intermediate language. We show results confirming the accuracy of our cost model by validating it on different scientific kernels. A case study is presented to demonstrate that a solution

*Corresponding author

Email addresses: `syed.nabi@glasgow.ac.uk` (Syed Waqar Nabi),
`wim.vanderbauwhede@glasgow.ac.uk` (Wim Vanderbauwhede)

created from our optimizing framework outperforms commercial high-level synthesis tools both in terms of throughput and power efficiency.

Keywords: performance model, cost model, high-performance computing, FPGA, high-level programming, high-level synthesis, roofline model

1. Introduction

Higher logic capacity and maturing high-level synthesis (HLS) tools are drivers to mainstream adoption of FPGAs in high-performance computing (HPC) and big data. The fine-grained flexibility of an FPGA comes with the challenge of figuring out and programming the best architecture for a given scientific kernel. HLS tools like Maxeler[1], Altera OpenCL[2], Xilinx SDAccel[3] and LegUp[4] have raised the abstraction of design entry considerably and made it easier to program FPGAs. Parallel programmers with domain expertise are however still needed to fine-tune the application for performance and efficiency. “Portable” heterogeneous frameworks like OpenCL are playing an important role in making heterogeneous computing more accessible, but they are not *performance*-portable across devices [5]. The performance portability issue is all the more acute with FPGAs. We contend that the design flow for HPC needs to evolve beyond current HLS approaches to address the productivity gap between the capacity of modern devices and our ability to efficiently program them. Our proposition is that for true performance portability, the design entry should be at a higher level of abstraction, and that the task of generating architecture-specific parallel code should be done by the compilers

Our proposal is to allow design entry at a fundamental and generic abstraction, inspired by functional languages with expressive type systems like Haskell¹ or Idris². The resultant flow, which we call the *TyTra* flow, is based on *type-based program transformations* (or *type transformations* for short)

¹<http://www.haskell.org>

²<http://www.idris-lang.org/>

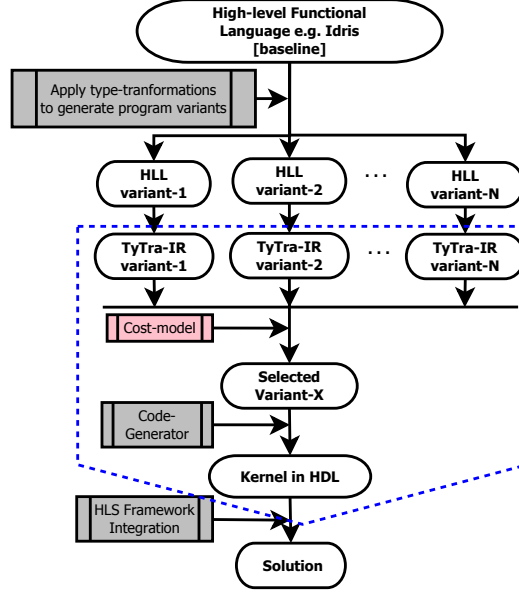


Figure 1: The TyTra design flow, showing design entry in a functional language, to an optimized FPGA solution. The dotted line marks the stages that are currently automated.

as shown in Figure 1. The design entry is at a pure software, *functional* abstraction, with no explicit parallel programming required by the user. We transfer the task of variant generation, search space exploration and converging on the optimal solution to the compiler. Program variants are generated using *type transformations* and translated to the TyTra intermediate language (IR). The compiler internally analyses the variants and emits code in a hardware description language (HDL), which is integrated with an existing HLS programming framework.

A key enabler of our approach is the performance and cost model embedded inside our flow, based on *roofline analysis* [6]. An automated search space explorer based on the roofline model is an entirely novel proposition to the best of our knowledge, and is the main contribution of this paper.

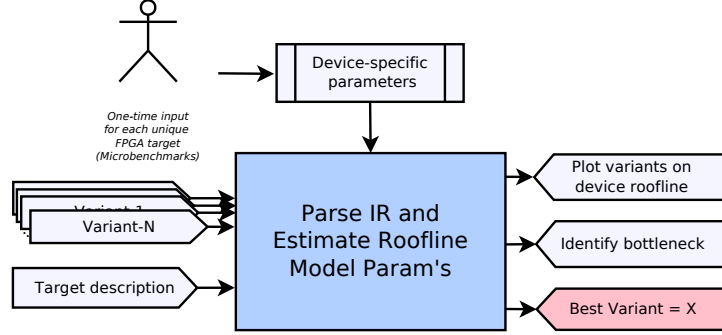


Figure 2: The use case of the cost model that is integrated inside the TyTra design flow.

36 The use case of our cost model is shown in Figure 2. A one-time set of
 37 synthetic micro-benchmark experiments are required for each new FPGA
 38 target. Then, given the IR descriptions of multiple, functionally equivalent
 39 design variants of a given kernel, we obtain estimates of their cost and per-
 40 formance on a roofline model, and pick the best performing variant from the
 41 search space. Note that the performance estimate on the roofline requires
 42 estimates of FPGA resource utilization and achievable memory bandwidth
 43 for each variant, and our methodology for calculating these estimates forms
 44 an important contribution of this work.

45 Our work is oriented towards the general area of high-performance sci-
 46 entific computing. Such applications are generally amenable to streaming,
 47 leading to pipelined implementations on FPGAs, and our framework is op-
 48 timized for this pattern. However, in principle, our approach is meant to be
 49 generic and comprehensive.

50 The rest of the paper is organized as follows: We first present the models
 51 of abstraction that we have developed or adopted in our framework. We
 52 then show how design variants are generated in the search space using *type*

53 *transformations*, and how these variants are represented in our custom IR.
 54 Next we present the *roofline analysis* model, followed by a section on how our
 55 IR based compilation approach allows us to quickly and accurately estimate
 56 the parameters required for the roofline analysis. We give an illustration of
 57 a comparative roofline analysis in the TyTra compiler, and an optimization
 58 case study using our approach. We finally present some related prior work
 59 before concluding the paper.

60 **2. Models of Abstraction in the TyTra Framework**

61 In general, we have adopted the models as defined in the OpenCL stan-
 62 dard [7] wherever possible, as this provides us with a familiar anchor, and
 63 suits our aim of eventually making our compiler work not just for FPGAs
 64 but for truly heterogeneous platforms.

65 *2.1. Platform and Memory Hierarchy Model*

66 The platform model, based on the OpenCL model, along with the memory
 67 model described later, is shown in Figure 3. The *Compute Unit* is the unit of
 68 execution for a kernel. The *Processing Element* (PE) is the custom datapath
 69 unit created for a given kernel, and may be considered equivalent to a pipeline
 70 *lane*, which may be *scaled* (i.e. replicated) for parallelism if there are enough
 71 resources on the FPGA.

72 As with the platform model, we adopt the OpenCL abstractions to de-
 73 scribe the memory hierarchy on the FPGA, also shown in Figure 3.

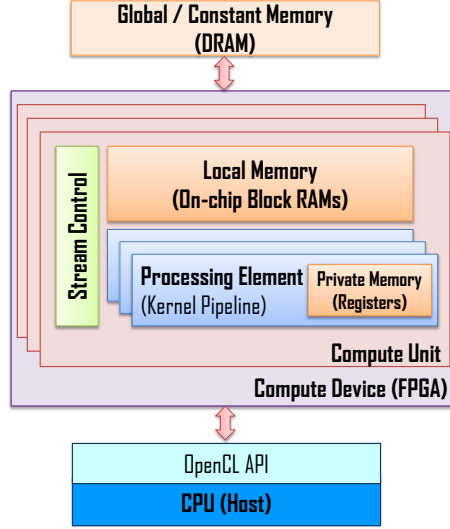


Figure 3: The TyTra platform and memory model. Both these models map OpenCL abstractions to the FPGA architecture.

74 2.2. Kernel Execution model

75 The execution model too is adopted from the OpenCL standard, us-
 76 ing terms like *kernel*, *work-item*, *work-group*, *NDRange*, *global-size*, *kernel-*
 77 *instance*. Readers are referred to the OpenCL standard [7] for definition of
 78 these terms.

79 2.3. Memory Execution Model

80 A typical host–device partitioned application can have different *forms*
 81 of execution with respect to data movement across the memory hierarchy,
 82 as multiple *kernel-instances*³ are executed. This *form* effects the achievable
 83 performance significantly. Hence, our framework requires a structured way
 84 of taking this into account when estimating performance.

³A kernel-instance is execution of the kernel for all *work-items* in the *NDRange*.

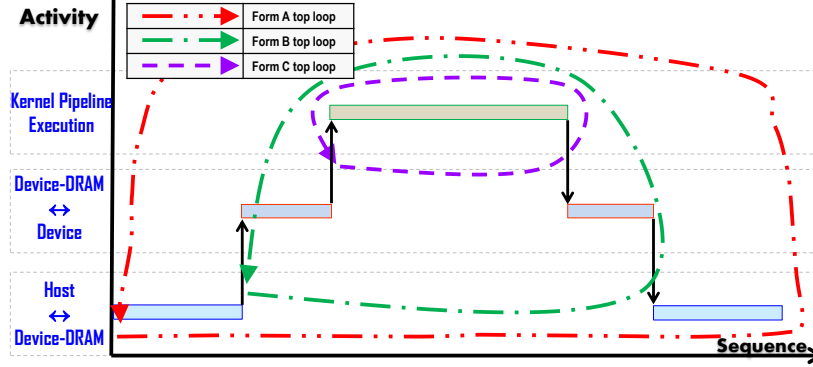


Figure 4: The three forms of execution based on how the memory hierarchy is traversed across multiple iterations of the top loop.

85 We have defined three forms of memory execution scenarios, which can
 86 be understood with reference the memory hierarchy (host \leftrightarrow device-DRAM
 87 \leftrightarrow device) and to Figure 4. *Form A* is where the top loop – the one that
 88 repeatedly executes the kernel over the entire index-space (generally the *time*
 89 loop in scientific applications) – is *outside* the host \leftrightarrow device-DRAM memory
 90 transfers, so these transfers take place on every iteration. A *Form B* ex-
 91 ecution is where the time loop is inside the host \leftrightarrow device-DRAM transfer,
 92 but outside the device-DRAM \leftrightarrow device transfer, so the host \leftrightarrow device-DRAM
 93 transfer happens only once. The iterations in a kernel-instance then access
 94 the data from the device-DRAM, i.e. the global memory. *Form C* is where
 95 the arrays for all work-items are small enough to fit inside the *local mem-*
 96 *ory*. In such a case, the time loop over the kernel-instance is inside both the
 97 host \leftrightarrow device-DRAM and device-DRAM \leftrightarrow device transfers⁴.

⁴We expect this model to evolve to take into account tiling the NDRange such that we can have a finer-grained spectrum between these three main forms.

98 2.4. Data Pattern Model

99 Streaming from the global memory is equivalent to looping over an ar-
100 ray. Since the pattern of index access has a significant impact on the sus-
101 tained bandwidth (see §6.3), this needs to be modelled. Our prototype model
102 currently considers two patterns: contiguous access and strided access with
103 constant strides. We plan to explore more sophisticated models in future
104 versions.

105 3. Generating Variants in the Search Space through Type Trans- 106 formations

107 A defining feature of our compiler is the generation of the search space by
108 creating *correct-by-construction* variants from a functional, high-level, base-
109 line description of a kernel through *type transformations*. Each program
110 variant will have a different cost and performance related to its degree of
111 parallelism. Using our roofline based cost model we can then select the best
112 suited instance in a guided optimisation search.

113 *Exemplar: Successive Over-Relaxation (SOR)*

114 We consider a SOR kernel, taken from the code for the Large Eddy Simu-
115 lator, an experimental weather simulator[8]. The kernel iteratively solves the
116 Poisson equation for the pressure. The main computation is a stencil over
117 the neighbouring cells (which is inherently parallel).

118 We express the algorithm in a functional language. Functional languages
119 can express higher-order functions, i.e. functions that take functions as
120 arguments and can return functions. They support *partial application* of

121 a function, and have strong type safety. These features make them suit-
 122 able as a high-level design entry point, and for generating safe or *correct-*
 123 *by-construction* program variants through type transformations. We use a
 124 dependently-typed functional language *Idris* because it supports dependent
 125 types which the type transformations require [9]. This feature is crucial for
 126 our purpose of generating program variants by reshaping data and ensuring
 127 correctness through type safety.

128 The baseline implementation of the SOR kernel in Idris is:

```
129 1  ps = map p_sor pps p rhs cn
```

130 p , rhs , and cn are the original vectors in the application, which are passed
 131 to the function pps that returns a *single* new vector equal to size of the 3D
 132 matrix $im.jm.km$. Each element of this vector is a *tuple* consisting of all
 133 terms required to compute the SOR, i.e. the pressure p at a given point,
 134 and its 6 neighbouring cardinal points, the weight coefficients cn and the rhs
 135 term for a given point.

136 Each tuple from this 3D matrix is passed to the computation kernel p_sor
 137 which computes the new value for the pressure:

```
138 1  p_sor pt = reltmp + p                                --'pt' is the tuple passed to p_sor
139 2                                                         --which then returns new pressure
140 3                                                         --based on original and delta
141 4  where
142 5  (p_i_pos,...,p,rhs) = pt                                --extract scalars from tuple 'pt'
143 6  reltmp = omega * (cn1 * (
144 7      cn2l * p_i_pos + cn2s * p_i_neg
145 8      + cn3l * p_j_pos + cn3s * p_j_neg
146 9      + cn4l * p_k_pos + cn4s * p_k_neg )
147 10      - rhs) - p                                --compute pressure delta 'reltmp'
```

148 The high-level function map performs computations on a vector without

149 using explicit iterators. So *map* applies *p_sor* to every element – which is
 150 a tuple – of the 3D matrix returned by *pps*, resulting in the new pressure
 151 vector *ps* of size *im.jm.km*.

152 Our purpose is to generate variants by transforming the *types* of the func-
 153 tions making up the program and *inferring* the program transformations from
 154 the type transformation. The details and proofs of the type transformations
 155 are available in [10]. In brief, we reshape the vector in an order and size pre-
 156 serving manner and infer the corresponding program that produces the same
 157 result. Each reshaped vector in a variant translates to a different arrange-
 158 ment of streams, over which different parallelism patterns can be applied.
 159 We then use our cost model to choose the best design.

160 As an illustration, assume that the type of the 1D-vector is *t* (i.e. an
 161 arbitrary type) and its size *im.jm.km*, which we can *transform* into e.g. a
 162 2-D vector with sizes *im.jm* and *km*:

```
163 1 pps : Vect (im*jm*km) t      --1D vector
164 2 ppst: Vect km (Vect im*jm t) --transformed 2D vector
165 3
```

166 Resulting in a corresponding change in the program:

```
167 1 ps  = map p_sor pps          --original program maps over 1D
168 2 ppst= reshapeTo km pps      --reshaping data
169 3 pst = map-par (map-pipe p_sor) ppst --new program with nested map over 2D
170 4                             --with parallelism annotation
```

171 where *map p_sor* is an example of *partial application*. Because *ppst* is
 172 a vector of vectors, the outer map takes a vector and applies the function
 173 *map p_sor* to this vector. This transformation results in a reshaping of the
 174 original streams into parallel *lanes* of streams, implying a configuration of
 175 parallel processing elements (pipelines) in the FPGA. Such a transformation
 176 is visualized in Figure 5.

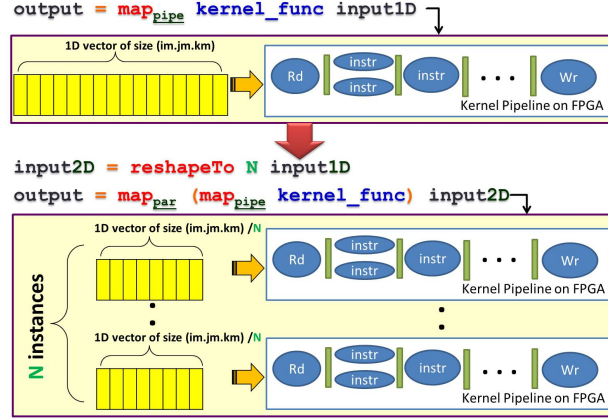


Figure 5: Using type transformations like *reshapeTo*, a baseline program which represents processing all $im.jm.km$ items in a single pipeline fashion (top) is converted to a program that represents N concurrent pipelines, each now processing $(im.jm.km)/N$ elements.

177 By applying different combinations of parallelism keywords *pipe*, *par* and
 178 *seq*, and reshaping along different dimensions, the search space very quickly
 179 explodes even on the basis of a single basic *reshape* transformation. Devel-
 180 oping a structured, accurate and fast evaluation approach is a key challenge
 181 of our approach.

182 4. Expressing Designs in the TyTra Intermediate Representation 183 Language

184 The high-level description of the application kernel as described in sec-
 185 tion 3 and not directly costable. Generating and then costing HDL code
 186 through synthesis and place-and-route on the other hand is too time-consuming.
 187 Our approach is to define an Intermediate Representation (IR) language,
 188 which we call the *TyTra-IR*. With reference to Figure 1, the TyTra-IR cap-
 189 tures the design variants generated by the front-end type transformations,

190 which can then be costed. The IR has semantics that can express the plat-
 191 form, memory, execution, design space and streaming data pattern models
 192 described in the previous section.

193 The TyTra-IR is used to express the device-side code only, and models
 194 all computations on a dataflow machine rather than a von-Neumann archi-
 195 tecture. The host-device interactions are managed by using the *shell* of a
 196 commercial HLS tool around the TyTra generated *kernel*.

197 The TyTra-IR is strongly and statically typed, and all computations are
 198 expressed using static single assignments (SSA). The compute language com-
 199 ponent and syntax are based on the LLVM IR [11], with extensions for co-
 200 ordination, memory access and parallelism. It has two components: the
 201 *Manage-IR* and the *Compute-IR*. The *Manage-IR* has semantics to instanti-
 202 ate *memory objects*, entities that can be the source or sink for a stream. Typ-
 203 ically, a memory object’s equivalent in software would be an array. *Stream*
 204 *objects* are used to express the connection between a processing element and
 205 a *memory object*.

<pre> ;1. Pipeline with ; combinatorial blocks pipe { instr instr combA() ... } ;2. Data-parallel ; pipelines par { pipeA() pipeA() ... } </pre>	<pre> ;3. Coarse-grained ; pipeline pipe { pipeA() pipeB() ... } ;4. Data-parallel ; Coarse-grained pipeline par { pipeTop() pipeTop() ... } ;where pipeTop{ pipeA() pipeB() ... } </pre>
---	--

Figure 6: Design configurations in the IR currently supported by the TyTra compiler.

206 The *Compute-IR* describes the PE(s), which typically is a pipelined im-
 207 plementation of the kernel datapath. The PEs are constructed by creating a
 208 hierarchy of *functions*, which may be considered equivalent to *modules* in an
 209 HDL like Verilog. However, these *functions* are described at a higher abstrac-
 210 tion than HDL, with a keyword specifying the parallelism for the function.
 211 These keywords are: **pipe** (pipeline parallelism), **par** (thread parallelism),
 212 **seq** (sequential execution) and **comb** (a custom combinatorial block). By
 213 using different parent-child and peer-peer combinations of functions of these
 214 four types, we can practically capture the entire search space for an FPGA
 215 target. The currently supported set of configurations shown in Figure 6 are
 216 those suitable for our application use case, i.e. HPC applications amenable to
 streaming, pipelined implementation on FPGAs. As an illustration, Figure 7

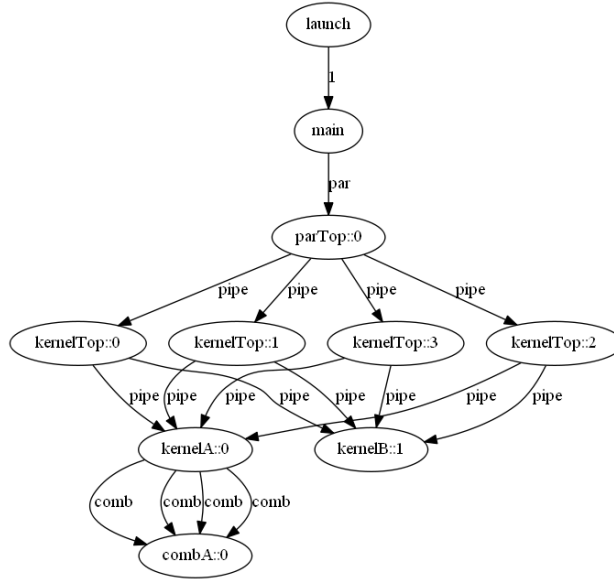


Figure 7: A typical configuration generated by the TyTra compiler showing a coarse-grained pipeline where one of the peer kernels uses a custom combinatorial function

218 shows the configuration tree created for multiple lanes of a coarse-grained
 219 pipeline where one of the peer kernels uses a custom combinatorial block.

220 5. Roofline Analysis for Evaluating Variants in the Search Space

221 Given such a framework as just described for representing design variants,
 222 the crucial requirement is being able to evaluate these variants for cost and
 223 performance. We use the *roofline* model inside our automated compiler as a
 224 systematic framework for evaluating design variants in the search space. Also,
 225 as it is a very visual performance model, it is useful for manual optimizations.

226 The roofline analysis [6] was introduced as a model to estimate the perfor-
 227 mance of a particular application on a multicore architectures. Since then, it
 228 has been adopted for GPUs [12] as well as FPGAs [13]. The model was
 229 based on the observation that “For the foreseeable future, off-chip memory
 230 bandwidth will often be the constraining resource in system performance”.
 231 The architectural constraints are captured by two *rooflines*, one representing
 232 the achievable *Computational Performance* (CP), and the other represent-
 233 ing the reachable memory bandwidth (BW). These rooflines are plotted on
 234 a plot of performance (GFLOPS/sec) vs operational or *computational in-*
 235 *tensity*(CI), which is defined as FLOPS per byte of *DRAM* traffic. The CI
 236 captures an algorithmic feature, that is, it predicts the DRAM bandwidth
 237 needed by a kernel. The proposed model brings together two architectural
 238 features – computational performance and memory performance – and one
 239 algorithmic feature, the computational intensity. The performance of a kernel
 240 is defined in the model as follows (shown visually in Figure 8):

$$241 \quad \textit{Attainable Performance}(\textit{FLOPS/sec}) = \min(\textit{CP}, \textit{BW} \cdot \textit{CI})$$

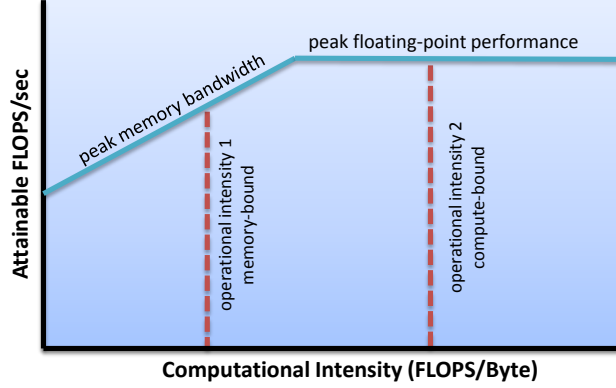


Figure 8: The original roofline model [6], showing a memory-bound and a compute-bound kernel.

242 5.1. Roofline Model for FPGAs

243 Silva et. al. [13] presented their extended roofline model for FPGAs.
 244 They observed that the straightforward approach of fixed rooflines that are
 245 hardware dependant no longer works for FPGAs. On FPGAs, the algorithm
 246 itself defines the architecture, and hence the rooflines for both the compu-
 247 tation and the memory bandwidth have to be adapted for each algorithm.
 248 Also, instead of floating-point operations, they use byte operations (BOPS)
 249 as more suitable for FPGA targets.

250 They also add the *scalability* parameter (SC), which captures the repli-
 251 cation of the PE. This scalability is determined by the available resources on
 252 the FPGA. The scalability (SC) is defined as:

$$253 \quad SC = \text{Available-resources} / \text{Resource-consumption-per-PE}$$

254 Hence the performance roof becomes:

$$255 \quad CP_{FPGA} = CP_{PE} \cdot SC$$

256 And the attainable performance:

$$257 \quad \textit{Attainable Performance}(BOPS) = \min(CP_{PE} \cdot SC, CI \cdot BW)$$

258 6. Roofline Analysis in the TyTra Flow

259 We have developed a prototype compiler that can parse the TyTra-IR
 260 of a design variant, and plot its performance on the roofline model. The
 261 compiler can also emit synthesizable HDL code for the kernel pipeline (see
 262 use case diagram in Figure 2). Our cost model for estimating the variables
 263 in the roofline model is primarily an empirical model, described as follows
 264 in the context of the roofline analysis model and the models developed in
 265 section 2.

266 6.1. Estimating Roofline Analysis Parameters in the TyTra Flow

Our starting point was the expression developed in [13] for the attainable performance on FPGAs:

$$\textit{Attainable Performance}(BOPS) = \min(CP_{PE} \cdot SC, CI \cdot BW) \quad (1)$$

267 Our main contribution is in how we estimate the four variables in Equation 1.
 268 In our framework, they are calculated on the basis of a set of parameters that
 269 depend on the target device, the kernel, and its design variant. Table 1 lists
 270 all these parameters, their key dependence (program, target hardware, design
 271 variant) and how we evaluate them in the TyTra compiler framework.

272 *Device Peak Computational Performance: CP_{PEAK}*

273 The horizontal *roof* in the roofline model refers to the peak computational
 274 capacity of the device, which is typically provided by the vendors. However,
 275 the FPGA adaptation of the model presented in [13] replaces this fixed roof

Param'	Description	Key Dependence	Evaluation Method
N_{GS}	Global-size of work-items in NDRange	Kernel	Parsing IR
N_{WOPK}	Word operations per kernel	Kernel	Parsing IR
N_{BPW}	Bytes per word	Kernel	Parsing IR
N_{OFF}	Maximum offset in a stream	Kernel	Parsing IR
K_{PD}	Pipeline depth of kernel	Design-variant	Parsing IR
F_D	Device's operating frequency	Design-variant and device	Parsing IR
L_{PI}	Latency per instruction	Design-variant	Parsing IR
N_I	Instructions per PE	Design-variant	Parsing IR
D_V	Degree of pipeline vectorization	Design-variant	Parsing IR
N_{WPT}	Words per memory I/O tuple	Kernel	Parsing IR
Max_X	Maximum available resource of type X	Target device	Architecture description
$Util_X$	Utilization of resource of type X	Design-variant	Parsing IR

Table 1: The parameters required to calculate the four main variables of the roofline model, along with their key dependence, and the way they are evaluated in the TyTra compiler.

276 with a dynamic one that depends on the algorithm in addition to the device.
277 The *roof* in their work is determined by the CP of one PE, scaled to the
278 maximum possible in that device, and we work with their definition:

$$CP_{PEAK} = CP_{PE} \cdot SC \quad (2)$$

279 *Computational Performance of one PE: CP_{PE}*

280 We have developed an expression for CP_{PE} that is generic enough to
 281 accommodate the various configurations that can be created on an FPGA.

We started from the basic definition of the computational performance for one PE, CP_{PE} , which is:

$$CP_{PE} = \frac{\text{total bytes executed per kernel instance}}{\text{time taken}} \quad (3)$$

This expression can be expanded based on the parameters described in Table 1:

$$CP_{PE} = \frac{N_{GS} \cdot N_{WOPK} \cdot N_{BPW}}{\frac{N_{OFF} + K_{PD}}{F_D} + \frac{N_{GS} \cdot L_{PI} \cdot N_I}{F_D \cdot D_V}} \quad (4)$$

282 The numerator is the total number of byte operations in the kernel-instance.
 283 The first term of the denominator is the time taken to fill offset buffers and
 284 the kernel pipeline. Then the second term accounts for the time taken to
 285 execute all work-items given that the offset buffers and pipelines were full.

286 For most applications where $N_{GS} \gg N_{OFF} + K_{PD}$, we can use the asymptotic
 287 performance by ignoring the time taken to fill offset buffers and kernel
 288 pipeline in Equation 4. This gives us the simplified expression:

$$CP_{PE} = \frac{F_D \cdot N_{WOPK} \cdot N_{BPW} \cdot D_V}{L_{PI} \cdot N_I} \quad (5)$$

289 *Processing Element Scaling: SC*

290 We restrict the scaling SC of the PE up to 80% utilization of any of the
 291 four FPGA resources, as 100% utilization of FPGAs is generally not possible
 292 [14]. We need an estimate of device utilization by the kernel PE as well as the
 293 *base platform* peripheral logic. This is taken up in §6.2. Once we have these

estimates, the scaling is determined by whichever one of the four resources on the FPGA runs out first:

$$SC = \min(\frac{Max_{LE}}{Util_{LE}}, \frac{Max_{FF}}{Util_{FF}}, \frac{Max_{DSP}}{Util_{DSP}}, \frac{Max_{RAM}}{Util_{RAM}}) \quad (6)$$

Maximum Attainable Bandwidth: BW

The *peak* bandwidth to host and global memory is typically available from vendor datasheets. However, an estimate of *achievable* memory bandwidth is more relevant, and a must for the roofline model. This is especially relevant in FPGAs where the performance tends to be *memory-bound* (see Figure 8). The distinction of forms of memory execution as presented in §2.3 is relevant here. *Form B* is the most common pattern, where the bandwidth of concern would be the DRAM (global memory) bandwidth. Our approach for making this estimate is discussed in §6.3.

Computational Intensity: CI

This is a critical parameter of the model that ties characteristics of the algorithm to the architecture. In our framework, it is straightforward to calculate it from the parameters available to us inside our framework:

$$CI = \frac{N_{WOPK}}{N_{WPT}} \quad (7)$$

We have now presented our approach to calculating all four terms in Equation 1 needed to estimate the *attainable performance*. Two aspects however need further elaboration and are discussed following: estimating device utilization (to calculate the scaling factor *SC*), and achievable bandwidth to the DRAM.

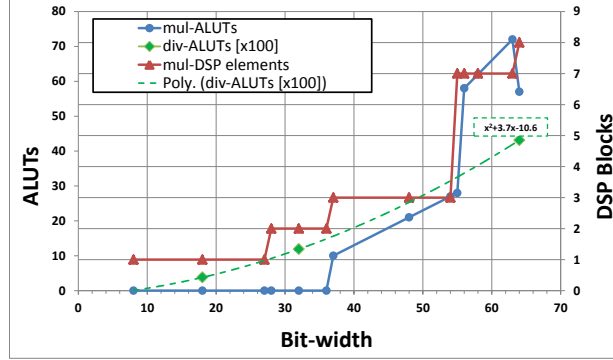


Figure 9: ALUTs used in unsigned integer division (see polynomial regression), and ALUTs and DSP-elements used in unsigned integer multiplication, on a Stratix-V device.

6.2. Resource-Utilization Cost Model

The scaling of a PE, and even the question of whether or not a single PE can fit in the FPGA, is determined by the available on-chip logic and memory resources. The resources are taken up by (1) the kernel PE, and (2) the peripheral logic or *base platform* that connects this PE to the memories via data streams.

6.2.1. Estimating Kernel PE Resource Utilization

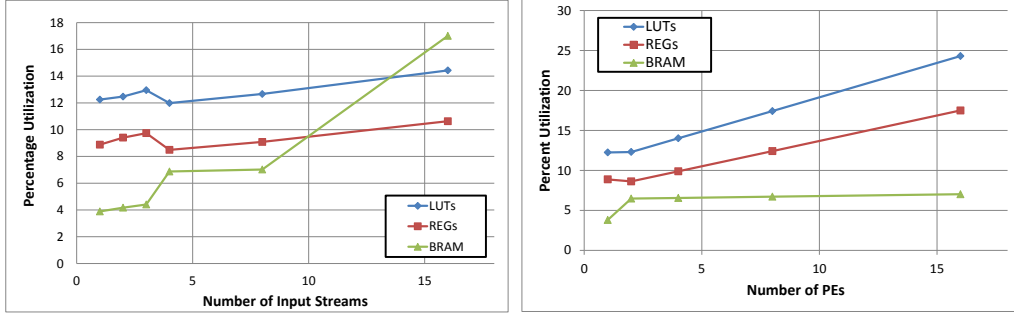
Our observation is that the regularity of FPGA fabric allows a simple empirical model to be built for most primitive instructions. As an example, consider the trend-line for LUT requirements against bit-width for integer division shown in Figure 9. It was generated from 3 data points (18, 32 and 64 bits) from micro-benchmark experiments on an Altera Stratix-V device. We can now use it for polynomial regression and interpolation, e.g., for 24 bits, and get an estimate of 654 LUTs, which compares favourably with the actual figure of 652 LUTs. A multiplier requires two different kinds of

resources: DSP-elements and LUTs. Both these resources show a piece-wise-linear behaviour with respect to the bit-width, with clearly identifiable points of discontinuity, also shown in Figure 9. This results in a relatively trivial empirical model. Other primitive IR instructions have similar or simpler expressions that we can use to estimate their resource utilization. We thus calculate the overall resource cost of the kernel by accumulating the cost of individual IR instructions and the structural information implied in the *type* of each IR *function*. With reference to Figure 7, if a kernel is identified as a *pipe*, then each of its instruction requires dedicated resource on the FPGA, along with pipeline registers. If we have a *par* function with child *pipe* functions, then each of the children requires dedicated logic resources.

6.2.2. Estimating Base Platform Resource Utilization

An estimate of the overhead of the peripheral logic or *shell* provided by a vendor *base platform* is crucial if we want to estimate the maximum scaling. For small kernels especially, this will dominate the resource consumption. This estimate is somewhat tricky however as the internal structure of the base platform is not visible to us.

Our use-case of primarily interfacing with the host or DRAM via data streams simplifies this estimate. We have designed a simple micro-benchmark the Altera OpenCL base platform where we instantiate a minimalist pass-through kernel, and synthesize the shell with varying the number of streams or varying number of PEs. Linear regression gives us the expressions we can insert into our compiler for generating the resource estimates of the shell, which are then added to the estimates of the kernel. The total resource utilization estimates are then used by our compiler for calculating the maximum



(a) For different number of input streams. (b) For different values of PE scaling (1 input stream in all cases).

Figure 10: The resource cost of the base-platform that creates streams feeding the TyTra-generated PE. One output stream in all cases, and word-size is 32 bits. Target is a Stratix-V device programmed with Altera-OpenCL.

possible PE scaling for a given kernel.

Our solution for estimating the base platform resources is based on two observations: first, changing the number of input streams has a marginal impact on the utilization of registers and LUTs, but significant impact on the utilization of BRAM (See Figure 10a); second, scaling the PE has significant impact on the utilization of registers and LUTs, but marginal impact on that of the on-chip BRAM (See Figure 10b). We hence use simplifying assumptions⁵ to avoid the complete matrix of synthesis experiments (all possible combinations of number of PEs and streams). Since the kernel compilation is independent of the host array (stream) sizes, this has no impact on the

⁵Even with a $\pm 2\%$ margin of error, we can assume the register and LUT usage to be independent of number of input streams, and the BRAM usage to be independent of PE scaling (apart from one outlier).

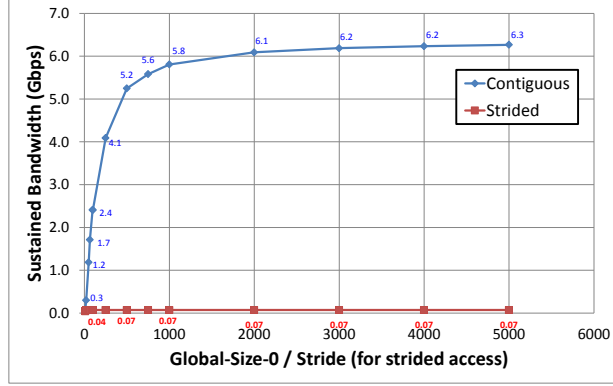


Figure 11: An empirical model of the dependency of sustained bandwidth on data size and contiguity of data, based on 32-bit integers. The horizontal axis represents one dimension of a square array, so it is also the stride in case of strided access. Results are based on Alpha-Data’s ADM-PCIE-7V3 board with a Xilinx Virtex 7 device. The performance can be improved with optimizations.

364 resource utilization of the base platform.

365 6.3. Estimating Sustained Memory Bandwidth

366 A significant variable in the throughput expressions is the bandwidth to
 367 the host or the device DRAM. While the *peak* bandwidth can easily be read
 368 off the datasheets, the *sustained* bandwidth for various streams in a particular
 369 design varies with the access pattern, size, and other parameters as well. We
 370 performed a set of experiments by extending the STREAM benchmark [15]
 371 to OpenCL, based on the work done in [16] for GPUs. Specifically, we tested
 372 the effect of having the data streams access data contiguously and in a strided
 373 manner, and changing the size of the streams and the strides. The results are
 374 shown in Figure 11. They highlight the importance of taking into account
 375 the factors effecting the sustained bandwidth for any realistic cost models.

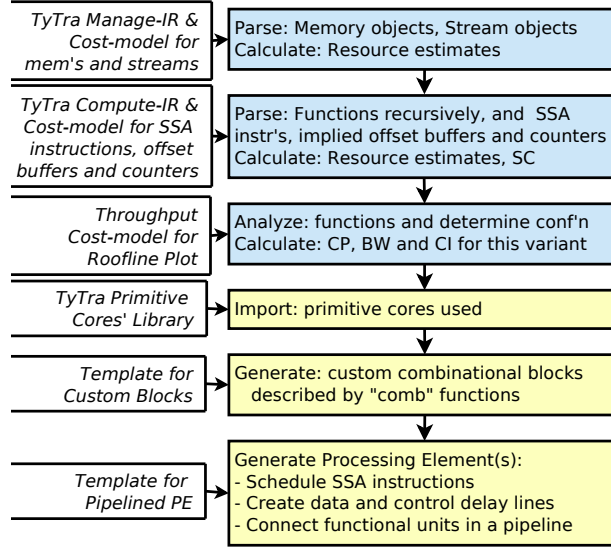


Figure 12: The TyTra back-end compiler flow, showing the estimation flow (blue/first three stages) and code generation flow (yellow). The starting point for this subset of the entire flow is the TyTra-IR description representing a particular design variant, ending in the generation of synthesizable HDL which can then be integrated with a HLS framework.

376 We have incorporated this empirical model into our compiler, and continue
377 developing the stream benchmark.

378 7. Using the Roofline Cost Model in the TyTra Compiler – an 379 Illustration

380 We have developed a prototype compiler that accepts a design variant
381 in TyTra-IR, estimates its cost and performance and plots it on the roofline
382 model, and if needed, generates the HDL code for it. The flow is shown in
383 Figure 12.

384 We created some design variants of the SOR kernel generated by type

```

1 ; **** COMPUTE-IR ****
2 @main.p = addrSpace(12) ui18,
3         !"istream", !"CONT", !0, !"strobj_p"
4 ;...[more inputs]...
5 define void @f0(...args...) pipe {
6     ;stream offsets
7     ui18 %pip1=ui18 %p, !offset, !+1
8     ui18 %pkn1=ui18 %p, !offset, !-ND1*ND2
9     ;...[more stream offsets]...
10    ;datapath instructions
11    ui18 %1 = mul ui18 %p_i_p1, %cn21
12    ui18 %2 = mul ui18 %p_i_n1, %cn2s
13    ;...[more instructions]...
14    ;reduction operation on global variable
15    ui18 @sorErrAcc=add ui18 %sorErr, %sorErrAcc
16 }
17 define void @main () {
18     call @f0(..args...) pipe }

```

```

1 ; **** COMPUTE-IR ****
2 @main.p0 = addrSpace(12) ui18,
3         !"istream", !"CONT", !0, !"strobj_p"
4 @main.p1 = ...
5 @main.p2 = ...
6 @main.p3 = ...
7 ;...[other inputs]...
8 define void @f0(...args...) pipe {...}
9 define void @f1 (...args...) par {
10     call @f0(...args...) pipe
11     call @f0(...args...) pipe
12     call @f0(...args...) pipe
13     call @f0(...args...) pipe }
14 define void @main () {
15     call @f1(..args...) par }

```

(a) Single PE.

(b) Scaled (x4) PEs.

Figure 13: Abbreviated TyTra-IR code for the two variants of the SOR kernel.

transformations as discussed in 3. Figure 13a shows the TyTra-IR for a the baseline configuration which is a single kernel-pipeline. The Manage-IR which declares the memory and stream objects is not shown.

Note the creation of offsets of input stream *p* in lines 6–9, which create streams for the six neighbouring elements of *p*. These offset streams, together with the input streams shown in lines 2–4 form the *input tuple* that is fed into the datapath pipeline described in lines 10–15. Figure 14 shows the realization of the kernel as a pipeline in the FPGA as generated by the TyTra compiler. The same SOR example can be expressed in the IR to represent *data parallelism* by adding multiple PE *lanes*, corresponding to a reshaped data along e.g four rows, by encapsulating multiple instances of the kernel-pipeline function shown in Figure 13a into a top-level function of type **par**, and creating multiple stream objects to service each of these parallel kernel-pipelines. This variant’s IR is shown in Figure 13b.

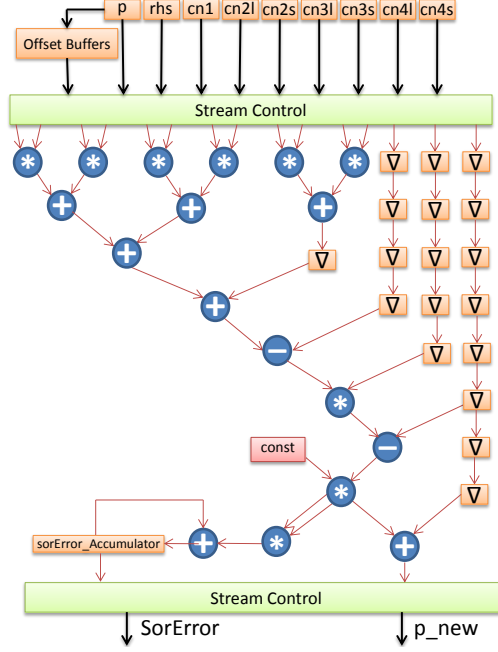


Figure 14: Pipelined datapath of the SOR kernel as generated by the TyTra compiler. Only pass-through pipeline buffers are shown; all functional units have pipeline buffers as well. The blocks at edges refer to on-chip memory.

7.1. Roofline Analysis of the Design Variants using our Cost Model

We use the high-level *reshapeTo* function to generate variants of the program by reshaping the data, which means we can take a single stream of size N and transform it into L streams of size $\frac{N}{L}$, where L is the number of concurrent lanes of execution in the corresponding design variant. This high level translation transforms to scaling the number of PEs.

Figure 15 shows the roofline plots of 5 variants thus generated. The first variant has a single PE, and the computational intensity CI intersects the computational roof CP_{PE} of the design. So this variant is *compute-bound*. With the performance well below the peak computational capacity of the

409 device for *this algorithm* (the blue dotted line), there is clearly room for
 410 improvement.

411 In the next variant, there are now 2 PEs, and since the design is still
 412 compute-bound, we see a proportional increase in performance. For the next
 413 variant, with PEs scaled to 4, the computational roof moves even further
 414 upwards, and we are almost at the intersection of compute and bandwidth
 415 roofs. This is the ideal situation as we are making the best use of both
 416 the available computation and bandwidth capabilities. One can predict that
 417 further scaling will not yield any improvement as the design moves into the
 418 memory-bound region. This is confirmed by the two more roofline graphs

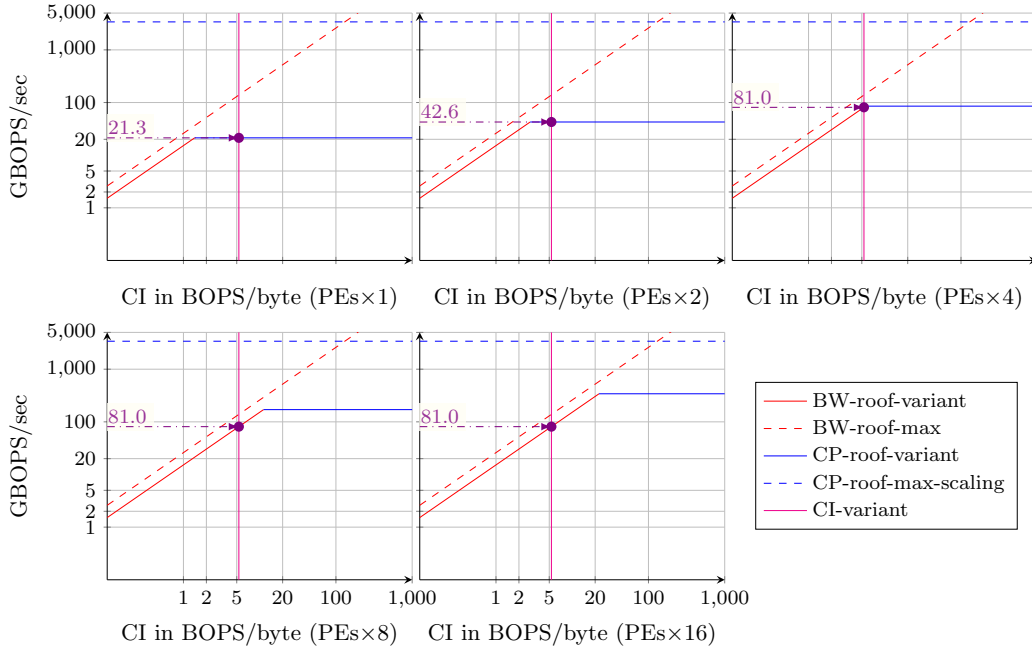


Figure 15: Evaluation of variants for the SOR kernel generated by applying the PE-scaling transformations. We get dividends from scaling until we hit the memory-wall at a scaling of 4.

419 showing the PEs scaled to 8 and 16 respectively, yet the performance con-
420 strained at what was estimated for a scaling of 4.

421 The limit of PE scaling itself is determined by our device utilization
422 model, and is used to determine the CP_{PEAK} (blue-dotted line). If we do
423 not encounter the memory roof first, we can in theory scale the PE until we
424 reach CP_{PEAK} .

425 We can see from the roofline plots that we can improve the performance
426 of this design by either improving the sustained bandwidth to the memory
427 which is still below peak, or by carrying out an algorithmic or memory buffer-
428 ing optimization that increases the computational intensity. If, for another
429 design, the limiting factor was CP_{PEAK} , then the optimization focus would
430 be on reducing device utilization, e.g. by using reduced precision arithmetic.

431 We would like to highlight here that the estimator is very fast: the current
432 implementation, although written in Perl, takes only 0.3 seconds to evalu-
433 ate one variant. This is more than $200\times$ faster than e.g. the preliminary
434 estimates generated by SDAccel which takes close to 70 seconds.

435 We would also like to point out that while the cost-model does facilitate
436 the evaluation of the search-space by providing a light-weight high-level route
437 to estimates, on its own it does not *simplify* the search-space. The issue of
438 simplifying the design search-space is important in its own right, as it can
439 very quickly explode to an unmanageable number even for relatively small
440 applications. We are currently working on an approach to simplify the search-
441 space, but that is outside the scope of this paper.

442 7.2. Accuracy of the cost model

443 Preliminary results on relatively small but realistic scientific kernels have
444 been very encouraging. We evaluated the estimated vs actual⁶ utilization
445 of resources for the kernel pipelines, and throughput measured in terms of
446 cycles-per-kernel-instance in Table 2. We tested the cost model by evaluating
447 the integer version of kernels from three HPC scientific applications: (1)
448 The successive over-relaxation kernel from the LES weather model that has
449 been discussed earlier; (2) The *hotspot* benchmark from the Rodinia HPC
450 benchmark suite [17], used to estimate processor temperature based on an
451 architectural floorplan and simulated power measurements; (3) The *lavaMD*
452 molecular dynamics application also from Rodinia, which calculates particle
453 potential and relocation due to mutual forces between particles within a large
454 3D space.

455 These results confirm that an IR defined at an appropriate abstraction
456 will allow quick estimates of cost and performance that are accurate enough
457 for relative comparison of design variants in the search space.

458 Currently our cost model has two limitations which we are investigating.
459 First, it does not anticipate the optimizations done in the relevant synthesis
460 tool. We will however require better visibility into the behaviour of synthe-
461 sis tools like Quartus if we are to have a realistic, nuanced model for such
462 synthesis optimizations, and we will explore this in the future. Secondly, the
463 accuracy we see in Table 2 is for the *kernel* estimates only. When we compare

⁶ The *actual* resource utilization figures are based on full synthesis, and *actual* cycle-counts are from RTL simulations. The design entry for these experiments is in Verilog RTL. The RTL is generated from TyTra-IR description using our back-end compiler.

Kernel		LUT	REG	BRAM	DSP	CPKI
Hotspot (Rodinia)	Estimated	391	1305	32.8K	12	262.3K
	Actual	408	1363	32.7K	12	262.1K
	% error	4	4.2	0.3	0	0.07
LavaMD (Rodinia)	Estimated	408	1496	0	26	111
	Actual	385	1557	0	23	115
	% error	6	3.9	0	13	3.4
SOR	Estimated	528	534	5418	0	292
	Actual	534	575	5400	0	308
	% error	1.1	7.1	0.3	0	5.2

Table 2: The estimated vs actual⁶ performance and utilization of resources, the former measured in terms of cycles-per-kernel-instance (CPKI), for the kernel of three scientific applications. Percentage errors also shown. All are executed as *Form-C* implementations (see §2.3).

464 the performance of a complete solution (kernel logic generated by tytra, shell
465 logic based commercial HLS tool) with the TyTra estimate, the accuracy is
466 relatively lower (see Figure 17), though we still achieve the primary purpose,
467 i.e., finding the best design variant.

468 8. Case Study: Comparison of a TyTra-generated solutions against 469 HLS tools

470 A working solution using an FPGA accelerator requires a base platform
471 or *shell* on the FPGA to deal with off-chip IO and other peripheral functions,
472 along with an API for accessing the FPGA accelerator. We use a commer-
473 cially available frameworks to implement this shell, and the TyTra-generated
474 HDL code for the kernel. We will now compare this *hybrid* approach against

475 the *baseline* using only the HLS tool, for two different frameworks.

476 Maxeler’s MaxJ [1] is an HLS design tool for FPGAs, and provides a Java
 477 meta-programming model for describing computation kernels and connecting
 478 data streams between them. The experimental setup for the experiments on
 the Maxeler framework is shown in Figure 16.

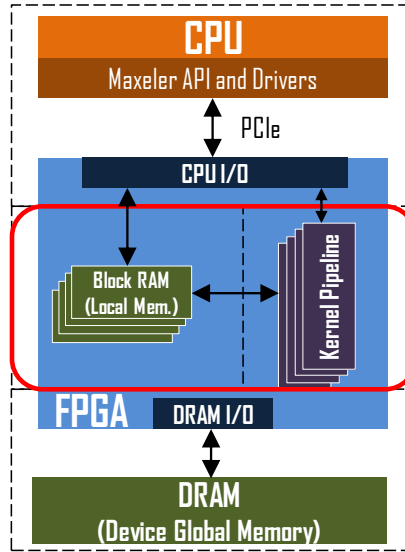


Figure 16: The Maxeler-TyBEC hybrid solution. The dotted line identifies what is programmed using the Maxeler HLS tool (shell). The solid/red line identifies the logic programmed with TyTra generated code (kernel). The overlap indicates that stream generation from on-chip Block-RAMs can be done by either.

479

480 The CPU implementation (*cpu*) is compiled with `gfortran -O2`. The
 481 first FPGA implementation is using only the Maxeler flow (*fpga-maxJ*),
 482 which incorporates pipeline parallelism automatically extracted by the Max-
 483 eler compiler. The second FPGA implementation (*fpga-tytra*) is the design
 484 variant generated by the TyTra back-end compiler, based on a high-level type
 485 transformation that introduced parallelism ($4\times$ PEs) in addition to pipeline

parallelism. We collected results for different dimensions of the input 3D arrays, i.e. `im`, `jm`, `km`, ranging from 24 elements along each dimension (55 KB) to 194 elements (57 MB). .

8.1. Performance Comparison

The performance comparison of Maxeler-only (*fpga-maxJ*) and Maxeler-TyTra hybrid (*fpga-tytra*) is shown in Figure 17. Note that *fpga-maxJ* could in principle be optimized manually to achieve a similar performance as *fpga-tytra*, but we deliberately use an unoptimized baseline for *fpga-maxJ*. Our contention is that by using our approach, one can obviate the need to carry out manual optimizations in an HLS tool like Maxeler. Hence our competition is an unoptimized HLS solution.

Apart from the smallest grid-size, *fpga-tytra* consistently outperforms *fpga-maxJ* as well as *cpu*, showing up to $3.9\times$ and $2.6\times$ improvement over *fpga-maxJ* and *cpu* respectively. At small grid-sizes though, the overhead of handling multiple streams per input and output array dominates and we have relatively less improvement or even a decrease in performance. In general, FPGA solutions tend to perform much better than CPU at large dimensions.

An interesting point to note for comparison against the baseline CPU performance is that at the typical grid-size where this kernel is used in weather models (around 100 elements / dimension), the *fpga-maxJ* version is *slower* than *cpu*, but *fpga-tytra* is $2.75\times$ faster. These performance results clearly indicate that a straightforward implementation on an HLS tool will not be optimal and manual effort would be required; the TyTra flow can automate this.

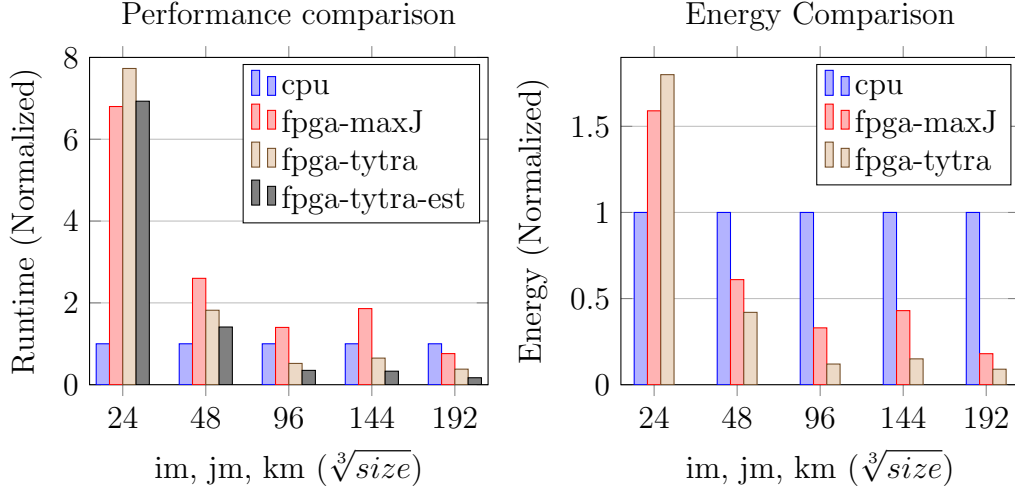


Figure 17: Comparing performance and energy differential of the SOR kernel for different sizes of grid, normalized against the CPU-only solution. The figures are for 1000 iterations of the kernel. Setup: Intel-i7 quad-core processor at 1.6GHz, 32 GB RAM, and an Altera Stratix-V-GSD8 FPGA.

510 If we look at the (the *fpga-tytra-est* column) showing the performance pre-
511 dicted by our cost model, we can see they are not accurate as the kernel-only
512 estimates in Table 2. The introduction of the shell adds a degree of inaccu-
513 racy to the performance estimate, which in the worst case in this particular
514 example is off by $2.35\times$. However, the use-case of finding the best variant
515 from a search-space is still very much applicable as these results show.

516 To further qualify our approach, we compared it against another com-
517 mercial HLS tool, Altera-OpenCL (AOCL), using a 2D SOR kernel. The
518 run-time, normalized against a baseline CPU implementation⁷, is shown in

⁷A faster Xeon CPU along with higher data locality for 2D stencil would explain why the CPU performs much better than the FPGA in this experiment, as compared to the

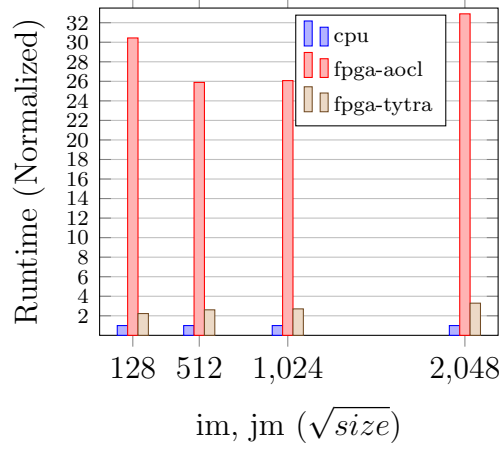


Figure 18: Runtime of the 2D-SOR kernel for AOCL-only and AOCL-TyTra hybrid for different sizes of grid, normalized against the CPU-only solution. Setup: Intel Xeon E5 quad-core at 2.4 GHz, 64GB RAM, and an Altera Stratix-V-GSD5 FPGA.

519 Figure 18.

520 The advantage of our approach to FPGA programming is starkly demon-
521 strated in this experiment, where – using an approach similar to the one
522 described for the Maxeler-TyTra experiment – the Tytra solution (with an
523 AOCL shell) yields an order of magnitude better performance than the
524 AOCL-only solution on the same FPGA⁸.

one on Maxeler.

⁸As opposed to the *fpga-tytra* or the *fpga-maxj* solution, we were unable to use on-chip buffers for stencil data in the *fpga-aocl* solution, as AOCL failed to synthesize within available resources (see Figure 19). Hence the *fpga-aocl* solution accesses the main memory for every data-point in the stencil, which affects its performance.

525 8.2. Energy Comparison

526 For the energy figures, we used the actual power consumption of the
527 host+device measured at the node’s power socket using a WattsUp power
528 meter. For a fair comparison, we noted the increase in power from the idle
529 CPU power, for both CPU-only and CPU-FPGA solutions. As shown in ??,
530 FPGAs very quickly overtake CPU-only solutions, and *fpga-tytra* solution
531 shows up to $11\times$ and $2.9\times$ power-efficiency improvement over *cpu* and *fpga-*
532 *maxJ* respectively. The energy comparison further demonstrates the utility
533 of adopting FPGAs in general for scientific kernels, and specifically our ap-
534 proach of using type transformations for finding the best design variant.

535 8.3. Resource Utilization Comparison

536 Previous results show the optimized hybrid TyTra solution compared with
537 baseline, unoptimized solutions using HLS tools. Here we compare what
538 happens when we compare like-for-like variants, that is the *same* optimization
539 using the two approaches, with the AOCL tool as the baseline. The results
540 are shown in Figure 19 ⁹ We also compare the effect of varying the array
541 sizes for both cases, which effect the size of internal buffers for stencil data,
542 and hence effect resource utilization.

543 We can see that the resource utilization is comparable for the baseline so-
544 lution with one PE. However, when we optimize the design by replicating the
545 PEs, then the AOCL-only solution – which implements the optimization by

⁹Full synthesis results are used, apart from cases where design could not synthesize because required resources exceeded availability, in which case we used estimated resources emitted by AOCL.

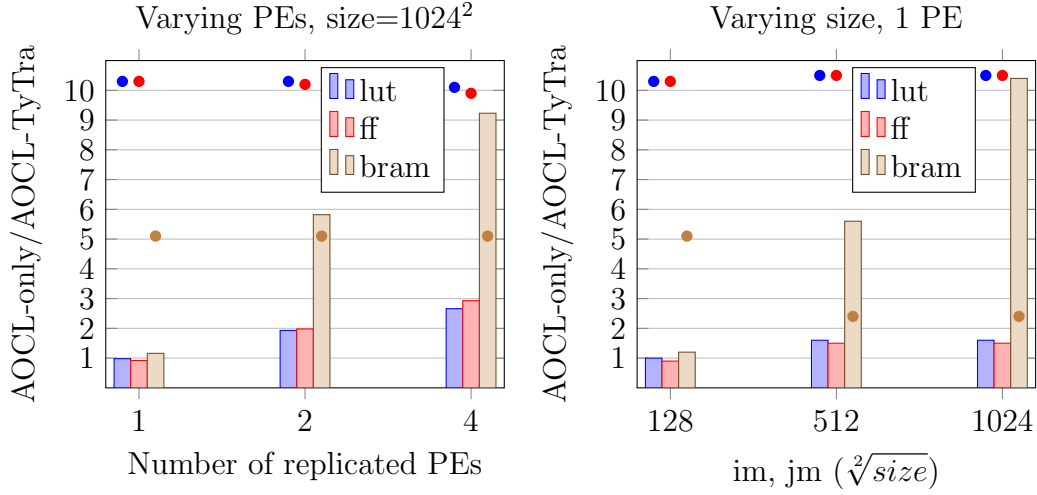


Figure 19: Normalized FPGA resource utilization, AOCL-only against AOCL-TyTra, for equivalent design variants. The dots represent maximum available resource, so if the dot is inside a plot, it means the required resource exceeds availability and did not synthesize.

546 changing the number of *compute-units* in the OpenCL code – takes up much
547 more resources than the AOCL-TyTra solution, especially in the utilization
548 of BRAMs. A similar observation is made for the case when we fix the design
549 to one PE, and change the size of data¹⁰. In fact, the AOCL-only solution
550 do not even synthesize in most cases as the available BRAM resources are
551 exceeded. These results make a strong case for using our flow not just to
552 generate or evaluate the variants, but also to *implement* them based on our
553 generated HDL code.

¹⁰We have found that the Maxeler framework is more efficient at using resources even when the PE-replication optimization is implemented entirely in Maxeler. However, that requires more programming effort as compared to simple pragma based optimization in AOCL.

554 9. Related Work

555 We can discuss related work from three different perspectives, i.e., in
556 relation to: raising the design-entry abstraction above conventional high-
557 level languages in general, high-level programming approaches specific to
558 FPGAs, and cost/performance models developed for FPGAs.

559 Our observation that there is a requirement for a higher abstraction de-
560 sign entry than conventional high-level languages is not novel in itself. For
561 example, researchers have proposed algorithmic skeletons to separate algo-
562 rithm from architecture-specific parallel programming [18]. SparkCL [19]
563 brings increasingly diverse architectures, including FPGAs, into the familiar
564 Apache Spark framework. Domain-specific languages (DSL) are another way
565 to raise the design abstraction within the scope of a particular application
566 domain, and numerous examples can be found for FPGAs. For example,
567 *FSMLanguage* for designing FSMs [20], and *CLICK* for networking applica-
568 tions [21].

569 There is considerable work that deals specifically with Programming FP-
570 GAs using conventional high-level programming. Such approaches raise the
571 abstraction of the design-entry from HDL to typically a C-type language, and
572 apply various optimizations to generate an HDL solution. Our observation
573 is that most solutions have one or more of these limitations that distinguish
574 our work from them: (1) design entry is in a *custom* high-level language,
575 that nevertheless is not a pure software language and requires knowledge
576 of target hardware and the programming framework [1, 2, 22], (2) compiler
577 optimizations are limited to improving the overall architecture already spec-
578 ified by the programmer, with no real *architectural* exploration [1, 2, 22, 4],

579 (3) solutions are based on creating a soft microprocessors on the FPGA and
 580 are not optimized for HPC [4, 23], (4) the exploration requires evaluation of
 581 variants that take a prohibitively long amount of time [22], or (5) the flow is
 582 limited to very specific application domain e.g. for image processing or DSP
 583 applications [24]. The *Geometry of Synthesis* project [25] is more similar
 584 than others, with its design entry in a functional paradigm and generation
 585 of RTL code for FPGAs, but does not include automatic generation and
 586 evaluation of architectural design variants as envisioned in our project. A
 587 flow with high-level, pure software design entry in the functional paradigm,
 588 that can apply *safe* transformations to generate variants automatically, and
 589 quickly evaluate them to achieve architectural optimizations, is to the best
 590 of our knowledge an entirely novel proposition.

591 Comparison with work related to cost models is another dimension. We
 592 have used the work described in [26] on extending the roofline analysis for
 593 FPGAs. However, our work is fundamentally different as we are only using
 594 the abstractions offered in the roofline analysis model; the manner in which
 595 we actually generate and represent variants, and estimate the cost param-
 596 eters are entirely novel contributions of our work. Kerr et. al. [27] have
 597 developed a performance model for CUDA kernels on GPUs based on em-
 598 pirical evaluation of a number of existing applications. Park et. al. [28]
 599 create a performance model for estimating the effects of loop transformation
 600 on FPGA designs. Since our *type transformations* can be viewed as a differ-
 601 ent abstraction for achieving similar outcomes, so there is a strong parallel
 602 between their work and ours. However, their work seems to focus on loop-
 603 unrolling, and is fundamentally different in terms of design entry and variant

604 generation. Dent et. al. presented cost models for area, time and power
 605 [29] which is based on the MATLAB-based *FANTOM* tool. Their approach
 606 of using an empirical model based on actual synthesis experiments resonates
 607 with our approach. However, their estimation model works on generated
 608 HDL whereas we make estimates at a higher abstraction, and our approach
 609 of generating and evaluating variants is fundamentally different. Reference
 610 [30] presents another cost estimation approach comparable to ours, where
 611 regression analysis is done on empirical data from synthesis tools to create
 612 resource estimation models, which are then used at compile-time on FPGA
 613 designs programmed at a high-level using the SA-C language. Their work
 614 does not estimate performance however, and the overall context is very dif-
 615 ferent from the TyTra flow. More recently, [31] have presented an analytical
 616 model, but their focus is on estimating dynamic and static power of various
 617 architectures.

618 **10. Conclusion**

619 FPGAs are increasingly being used in HPC for accelerating scientific com-
 620 putations. While the typical route to implementation is the use of HLS
 621 frameworks like Maxeler or OpenCL, they may not necessarily expose the
 622 parallelism opportunities on an FPGA in a straightforward manner. Tuning
 623 designs to exploit the available FPGA resources on these HLS tools is pos-
 624 sible but still requires considerable effort and expertise. We have presented
 625 an original flow that has a high-level design entry in a functional language,
 626 generates and evaluates design variants using a cost model on an intermedi-
 627 ate description of the kernel, and then emits HDL code. We have developed

628 abstractions used to create a structured cost model, and discussed our use
629 of the roofline model to automatically cost and evaluate design variants. We
630 have shown how our empirical approach to costing designs represented at an
631 intermediate level allows us to calculate all parameters required to plot the
632 performance of a design variant on the roofline model.

633 We have illustrated the use of our roofline-based cost model to evaluate
634 different variants of the SOR kernel. The accuracy of the cost model was
635 shown across three different kernels. A case study based on the SOR kernel
636 from a real-world weather model was used to demonstrate the high-level
637 type transformations. It was also used to give an illustration of a working
638 solution based on HDL code generated from our compiler, shown to give
639 better performance than the baseline solutions on both Maxeler and Altera-
640 OpenCL. In addition, we showed that even if the design optimizations were
641 to be programmed in the HLS tools, our approach gives much more efficient
642 resource utilization on the basis of its generated HDL code.

643 We are currently in the process of automating the generation of design
644 variants from high-level code. Also, we are working to extend our cost model
645 code generator to floating point as well more complex arithmetic operations.
646 We are also validating the cost model and code generator with larger and
647 more complex kernels, while expanding the set of available transformations.
648 Our approach to extending the cost-model is to keep evolving the TyTra-IR
649 as we experiment with more applications and transformations, and ensuring
650 the cost-model remains complete by providing an analytical or an empirical
651 model for all valid TyTra-IR instructions. Ultimately, our work aims to
652 provide a solution which has a high abstraction design entry, and in addition

will automatically converge on the best design variant from a single high-level description of the algorithm in a functional language. We are also working on evolving our flow to include legacy code written in languages typically used for scientific computing like Fortran or C.

Funding. This work was supported by EPSRC [grant number EP/L00058X/1].

[1] O. Pell, V. Averbukh, Maximum performance computing with dataflow engines, *Computing in Science Engineering* 14 (4) (2012) 98–103. doi:10.1109/MCSE.2012.78.

[2] T. Czajkowski, U. Aydonat, D. Denisenko, J. Freeman, M. Kinsner, D. Neto, J. Wong, P. Yiannacouras, D. Singh, From opencl to high-performance hardware on FPGAs, in: *Field Programmable Logic and Applications (FPL)*, 2012 22nd International Conference on, 2012, pp. 531–534. doi:10.1109/FPL.2012.6339272.

[3] The Xilinx SDAccel Development Environment (2014).
URL http://www.xilinx.com/publications/prod_mktg/sdx/sdaccel-backgroundunder.pdf

[4] A. Canis, J. Choi, M. Aldham, V. Zhang, A. Kammoona, J. H. Anderson, S. Brown, T. Czajkowski, Legup: High-level synthesis for FPGA-based processor/accelerator systems, in: *Proceedings of the 19th ACM/SIGDA International Symposium on FPGAs, FPGA '11*, ACM, New York, NY, USA, 2011, pp. 33–36.

[5] S. Rul, H. Vandierendonck, J. DHaene, K. De Bosschere, An experimental study on performance portability of opencl kernels, in: *Application*

- 676 Accelerators in High Performance Computing, 2010 Symposium, Papers,
677 2010.
- 678 [6] S. Williams, A. Waterman, D. Patterson, Roofline: An insightful visual
679 performance model for multicore architectures, Commun. ACM 52 (4)
680 (2009) 65–76. doi:10.1145/1498765.1498785.
681 URL <http://doi.acm.org/10.1145/1498765.1498785>
- 682 [7] The OpenCL Specification (2015).
683 URL <https://www.khronos.org/registry/cl/>
- 684 [8] C.-H. Moeng, A large-eddy-simulation model for the study of planetary
685 boundary-layer turbulence, J. Atmos. Sci. 41 (1984) 2052–2062.
- 686 [9] E. Brady, Idris, a general-purpose dependently typed programming lan-
687 guage: Design and implementation, Journal of Functional Programming
688 23 (2013) 552–593. doi:10.1017/S095679681300018X.
- 689 [10] W. Vanderbauwhede, Inferring Program Transformations from Type
690 Transformations for Partitioning of Ordered Sets (2015). arXiv:arXiv:
691 1504.05372.
692 URL <http://arxiv.org/abs/1504.05372>
- 693 [11] Chris Lattner and Vikram Adve, The LLVM Instruction Set and Compi-
694 lation Strategy, Tech. Report UIUCDCS-R-2002-2292, CS Dept., Univ.
695 of Illinois at Urbana-Champaign (Aug 2002).
- 696 [12] K.-H. Kim, K. Kim, Q.-H. Park, Performance analysis and opti-
697 mization of three-dimensional FDTD on GPU using roofline model,

- 698 Computer Physics Communications 182 (6) (2011) 1201 – 1207.
 699 doi:<http://dx.doi.org/10.1016/j.cpc.2011.01.025>.
 700 URL [http://www.sciencedirect.com/science/article/pii/](http://www.sciencedirect.com/science/article/pii/S0010465511000452)
 701 [S0010465511000452](http://www.sciencedirect.com/science/article/pii/S0010465511000452)
- 702 [13] B. da Silva, A. Braeken, E. H. D'Hollander, A. Touhafi, Performance
 703 modeling for fpgas: Extending the roofline model with high-level syn-
 704 thesis tools, Int. J. Reconfig. Comput. 2013 (2013) 7:7–7:7. doi:
 705 [10.1155/2013/428078](https://doi.org/10.1155/2013/428078).
 706 URL <http://dx.doi.org/10.1155/2013/428078>
- 707 [14] R. Tessier, H. Giza, Balancing logic utilization and area efficiency in fp-
 708 gas, in: Proceedings of the The Roadmap to Reconfigurable Computing,
 709 10th International Workshop on Field-Programmable Logic and Appli-
 710 cations, FPL '00, Springer-Verlag, London, UK, UK, 2000, pp. 535–544.
 711 URL <http://dl.acm.org/citation.cfm?id=647927.739548>
- 712 [15] J. D. McCalpin, Memory bandwidth and machine balance in current
 713 high performance computers, IEEE Computer Society Technical Com-
 714 mittee on Computer Architecture (TCCA) Newsletter (1995) 19–25.
- 715 [16] T. Deakin, S. McIntosh-Smith, Gpu-stream: Benchmarking the achiev-
 716 able memory bandwidth of graphics processing units, in: IEEE/ACM
 717 SuperComputing, Austin, United States, 2015.
- 718 [17] S. Che, M. Boyer, J. Meng, D. Tarjan, J. Sheaffer, S.-H. Lee, K. Skadron,
 719 Rodinia: A benchmark suite for heterogeneous computing, in: Workload

- 720 Characterization, 2009. IISWC 2009. IEEE International Symposium
721 on, 2009, pp. 44–54. doi:10.1109/IISWC.2009.5306797.
- 722 [18] M. Cole, Bringing skeletons out of the closet: a pragmatic manifesto for
723 skeletal parallel programming, *Parallel Computing* 30 (3) (2004) 389 –
724 406. doi:http://dx.doi.org/10.1016/j.parco.2003.12.002.
- 725 [19] O. Segal, P. Colangelo, N. Nasiri, Z. Qian, M. Margala, Sparkcl: A uni-
726 fied programming framework for accelerators on heterogeneous clusters,
727 CoRR abs/1505.01120.
- 728 [20] J. Agron, Domain-Specific Language for HW/SW Co-design for FPGAs,
729 Springer Berlin Heidelberg, Berlin, Heidelberg, 2009, pp. 262–284. doi:
730 10.1007/978-3-642-03034-5_13.
731 URL http://dx.doi.org/10.1007/978-3-642-03034-5_13
- 732 [21] C. Kulkarni, G. Brebner, G. Schelle, Mapping a domain specific lan-
733 guage to a platform fpga, in: *Proceedings of the 41st Annual Design*
734 *Automation Conference, DAC '04*, ACM, New York, NY, USA, 2004,
735 pp. 924–927. doi:10.1145/996566.996811.
736 URL http://doi.acm.org/10.1145/996566.996811
- 737 [22] J. e. a. Keinert, Systemcodesigner;an automatic esl synthesis approach
738 by design space exploration and behavioral synthesis for streaming appli-
739 cations, *ACM Trans. Des. Autom. Electron. Syst.* 14 (1) (2009) 1:1–1:23.
- 740 [23] K. Keutzer, K. Ravindran, N. Satish, Y. Jin, An automated explo-
741 ration framework for fpga-based soft multiprocessor systems, in: *Hard-*
742 *ware/Software Codesign and System Synthesis*, 2005. CODES+ISSS '05.

- 743 Third IEEE/ACM/IFIP International Conference on, 2005, pp. 273–
744 278. doi:10.1145/1084834.1084903.
- 745 [24] M. Kaul, R. Vemuri, S. Govindarajan, I. Ouais, An automated tem-
746 poral partitioning and loop fission approach for fpga based reconfig-
747 urable synthesis of dsp applications, in: Proceedings of the 36th Annual
748 ACM/IEEE Design Automation Conference, DAC '99, ACM, New York,
749 NY, USA, 1999, pp. 616–622. doi:10.1145/309847.310010.
- 750 [25] D. B. Thomas, S. T. Fleming, G. A. Constantinides, D. R. Ghica, Trans-
751 parent linking of compiled software and synthesized hardware, in: De-
752 sign, Automation Test in Europe Conference Exhibition (DATE), 2015,
753 2015, pp. 1084–1089.
- 754 [26] B. da Silva, A. Braeken, E. H. D'Hollander, A. Touhafi, Performance
755 modeling for FPGAs: Extending the roofline model with high-level syn-
756 thesis tools, International Journal of Reconfigurable Computingdoi:
757 10.1155/2013/428078.
- 758 [27] A. Kerr, G. Diamos, S. Yalamanchili, Modeling gpu-cpu workloads
759 and systems, in: Proceedings of the 3rd Workshop on General-Purpose
760 Computation on Graphics Processing Units, GPGPU 10, ACM, New
761 York, NY, USA, 2010, p. 3142. doi:http://doi.acm.org.prx.
762 library.gatech.edu/10.1145/1735688.1735696.
763 URL http://doi.acm.org.prx.library.gatech.edu/10.1145/
764 1735688.1735696
- 765 [28] J. Park, P. C. Diniz, K. R. S. Shayee, Performance and area modeling

- 766 of complete fpga designs in the presence of loop transformations, IEEE
767 Transactions on Computers 53 (11) (2004) 1420–1435. doi:10.1109/
768 TC.2004.101.
- 769 [29] L. Deng, K. Sobti, Y. Zhang, C. Chakrabarti, Accurate area, time and
770 power models for fpga-based implementations, Journal of Signal Pro-
771 cessing Systems 63 (1) (2011) 39–50.
- 772 [30] D. Kulkarni, W. A. Najjar, R. Rinker, F. J. Kurdahi, Compile-time area
773 estimation for lut-based fpgas, ACM Transactions on Design Automa-
774 tion of Electronic Systems (TODAES) 11 (1) (2006) 104–122.
- 775 [31] H. Mehri, B. Alizadeh, Analytical performance model for fpga-based
776 reconfigurable computing, Microprocessors and Microsystems 39 (8)
777 (2015) 796 – 806. doi:http://dx.doi.org/10.1016/j.micpro.2015.
778 09.009.